Monochromatic X-Ray Diffraction and Time-Resolved Measurements at High Pressure and Temperature

J. Chen (SUNY at Stony Brook)

Crystal structure refinements require accurate diffraction intensities. A monochromatic x-ray diffraction has many advantages over an energy dispersive diffraction for the accurate intensity measurements. Traditionally, high pressure *in situ* x-ray diffraction with a large-volume press was carried out in the energy dispersive mode (EDXD) because of the apparatus geometry. The pioneer attempt to acquire monochromatic x-ray diffraction with a large-volume press was made at the Photon Factory[1,2], however, the diffraction from sample surrounding materials remained as a problem for applying imaging plate (IP) detectors to the press. At beamline X17B1, we have developed a translating imaging plate system interfaced with large-volume press SAM85[3], and designed a new high pressure cell coupled with a subtraction data processing[4]. These developments first time allow us to perform time-resolved structure refinements at high pressure and temperature[5].

A experimental setup is schematically shown in Figure G-1. The imaging plates are mounted in a specially designed holder held on an optical rail. This can be tilted vertically and horizontally to the incident x-ray direction. The stage is movable along the incident x-ray direction to change the sample-to-IP distance (400 - 870 mm) and along the axis perpendicular to the incident x-ray beam for translating the IP during exposure. The holder can be easily taken off from the guide block to allow the goniometer arm to move down for EDXD measurements. A vacuum ensure two plates, either 200 mm x 250 mm or 200 x 400 mm size, are kept flat to the holder during exposure. When the imaging plate is used to record the diffraction pattern, the goniometer arm is rotated up to +35°. In the time-resolved measurements, a lead screen with a vertical slit in the middle is introduced in the front of the imaging plate to define the dimension of exposure on the detector. Width of the slit is adjusted

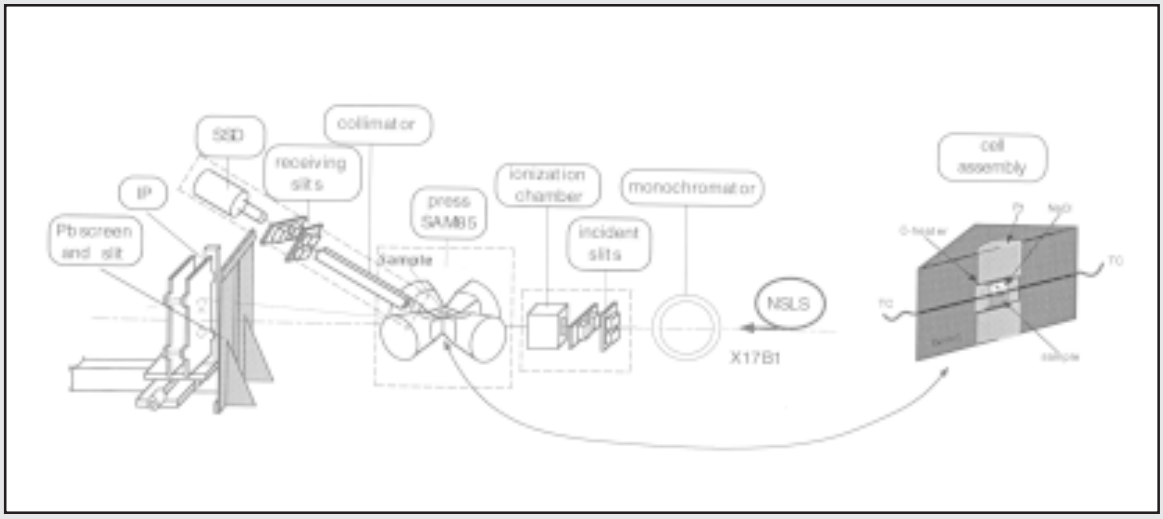

Figure G-1: Schematic layout of the translating imaging plate system for high P-T x-ray diffraction at the X17B1 beamline of the NSLS. The inset on the right shows the high-pressure cell assembly for the large-volume apparatus, SAM85. The monochromator is a Laue-Bragg double-crystal focusing monochromator.

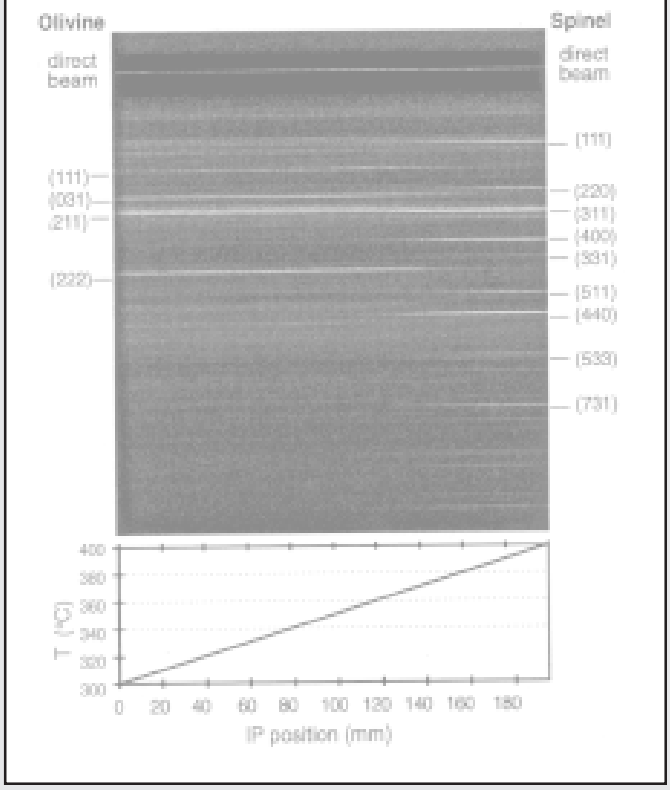

Figure G-2: Time resolved diffraction pattern on the imaging plate showing the olivine-spinel phase transition in fayalite at 5.9 GPa and 370°C. Left indices indicate the diffraction peaks of olivine phase; Right indices indicate those of spinel phase. Bottom curve shows the corresponding relation of sample temperature and imaging plate position.

depending on the beam intensity, IP-to-sample distance and the transporting speed of the imaging plate. A direct beam stop is mounted on the slit. The beam stop blocks most of the intensity of the direct beam, and allows the direct beam to expose the imaging plate with the same intensity as a diffracted beam.

The olivine-spinel transformation mechanism in fayalite was studied by the time-resolved diffraction measurements. The experiment was carried out by compressing the sample at room temperature into the spinel stability field (6.9 GPa) and then heating up the sample. The sample transformed from olivine to spinel during the heating. A time-resolved pattern was recorded when the temperature increased from 300°C to 400°C. The transporting speed of the imaging plate was 3.25mm/min. The heating rate was 1.75 °C/min. Figure G-2 shows the diffraction pattern taken with an 8 mm front slit and 0.2 mm x 0.2 mm incident x-ray beam. he photon energy of the x-ray was 41.12 keV and the sample-to-IP distance was 812.6 mm. In Figure G-2, the sample started with olivine phase (on the left) and ended up with spinel phase (on the right). Indices on the two sides of the pattern indicate major diffraction peaks of olivine and spinel phases respectively. Most of the intensity of the incident beam was blocked by a lead stop, with a thickness about 2 mm, behind the sample; the rest of the intensity made a direct beam marker on the top the imaging plate. Some high background (e.g. those close to spinel (111) peak) were from boron:epoxy pressure medium. The sample temperature was recorded as a function of imaging plate position and plotted at the bottom of Figure G-2. Thermal relaxation resulted in the pressure decrease from 6.9 GPa at room temperature to 5.7 GPa at 420°C. It is observed that the spinel phase started growing at 365°C and the olivine phase completely transformed into spinel at 390°C at about 5.9 GPa. Taking account the slit width, there is 52 mm on the imaging plate where the two phases coexist.

The diffraction pattern of two phase coexisting region on the IP was integrated as a function of time. After background subtraction, multi-phase structure refinements were make based on these date. Figure G-3 shows results of the sequence structure refinements. The emphasis of the refinements focused on the atomic occupancy in the spinel structure. All the occupancy parameters for Fe, Si and O were initially free for fitting. The refinements all resulted in the occupancy parameter for O close to 1. We therefore fixed the O occupancy to 1 for further refinements. The results showed that the occupancy parameters F_{si} and F_{fe} for Si and Fe are only 79% and 82% when the spinel phase is first recognized as amount of 20% of the mixture phases, and with growing of the spinel phase F_{si} and F_{fe} are increase rapidly. This observation indicates that the olivine-spinel transition involves the rearrangement of the oxide sub-lattice of hexagonally close-packed olivine, to form the cubic close-packed arrangement of the spinel structure, followed by the ordering of metals into the octahedral and tetrahedral voids.

Mechanism of the olivine-spinel phase transition has been investigated by several groups. Sung and Burns[6]

proposed a diffusion-controlled process, incoherent nucleation of the spinel phase and subsequent crystal growth; Kronberg [7] and Poirier[8] proposed a shear mechanism, stacking faults in oxygen lattice of olivine accompanying cation reordering coherently. More interesting result reported by Furnish and Bassett[9] from their observation of earlier appearance of some diffraction lines of spinel phase during the phase transition suggested a two-step shear mechanism with stacking faults prior to the cation reordering. However there was no sound evidence such as structure refinement to confirm any of these mechanisms. Our experiments first time provide the reliable data to support the two-step transformation mechanism. ■

Acknowledgments. All SAM85 team members have contributed to this work, and we wish to thank J. Hastings and P. Siddons at the NSLS for their technical support at the X17B1 beamline. The study is supported by the State University of New York at Stony Brook and the NSF Science and Technology Center for High Pressure Research (EAR 8920329). MPI pub. no. 225.

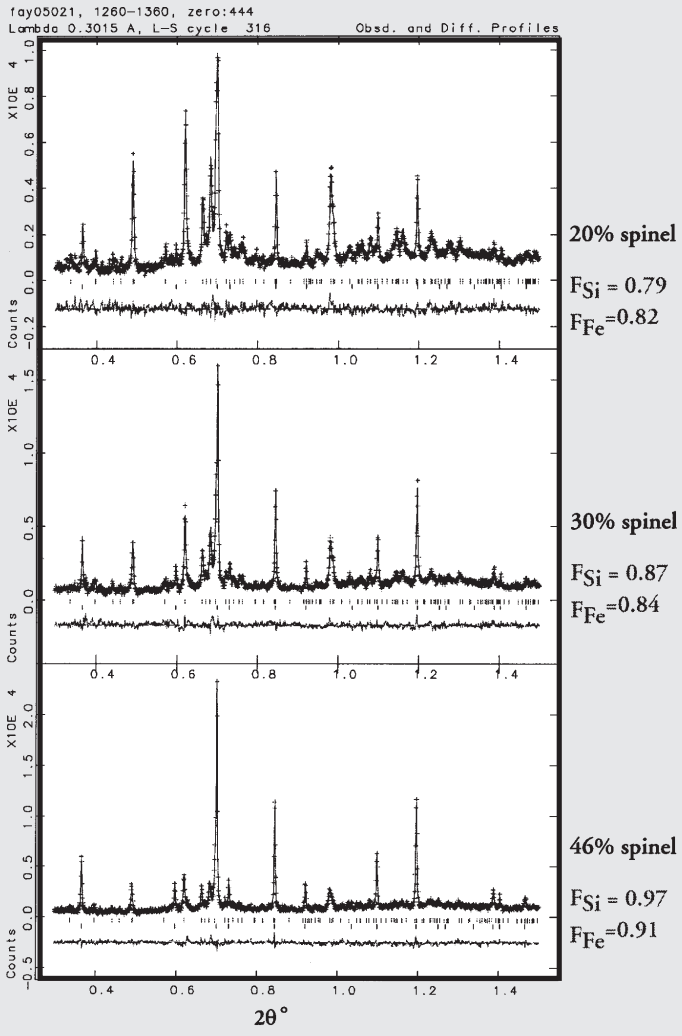

Figure G-3: Full Rietveld refinement of selected patterns in the time sequence through olivine-spinel transformation in fayalite.

[1] T. Kikegawa, J. Chen, Y. Kenichi, & O. Shimomura. *Rev. Sci. Instrum.* 66(2), 1335-1337(1995).
[2] J. Chen, T. Kikegawa, O. Shimomura and H. Iwasaki, *J. Synchrotron Rad.* 4, 21-27(1997).
[3] See abstract of the X17B1 beamline by J. Chen, D. J. Weidner, M. T. Vaughan, R. Li, J. B. Parise, C. C. Koleda and K. J. Baldwin in this report.
[4] J. Chen, J. B. Parise, R. Li, D. J. Weidner, and M. T. Vaughan, in *High-Pressure and Temperature Research: Properties of the Earth and Planetary Materials*, edited by M. H. Manghnani and T. Yagi, AGU Washington D.C., 1998, p129-134.
[5] See abstract of the X17B1 beamline by J. Chen and D. J. Weidner in this report.
[6] C. M. Sung and R. G. Burns, *Earth Planet. Sci. Lett.* 32, 165(1976).
[7] M. L. Kronberg, *Acta Metall.* 5, 507(1957).
[8] J. P. Poirier, in *Anelasticity in the Earth, Geodyn.* Ser. vol. 4, edited by F. D. Stacey *et al.* p. 113-117, AGU, Washington D.C. (1981).
[9] M. D. Furnish and W. A. Bassett, *J. Geophys. Res.* 88, 10333 (1983).

Synchrotron X-radiation, Ultrasonics, and the Composition of the Earth

M. T. Vaughan (Center for High Pressure Research, State University of New York at Stony Brook)

The primary data about the deep interior of the Earth that is relevant to its composition are the travel times of seismic waves. These data are used to determine the compressional and shear acoustic velocity and the density, as functions of depth. To determine the composition of the materials present there (in terms of both chemistry and phase), we need to measure in the laboratory the equivalent parameters of candidate earth materials at equivalent conditions of pressure and temperatures.

Acoustic velocities of many earth materials have been measured at elevated pressures and temperatures using ultrasonic interferometry for several decades now, however only recently have we been able to make these measurements at pressure and temperature conditions equivalent to the Transition Zone at 400 km. (~15 GPa)[1,2] . There has long been a problem of determination of the pressure in these experiments; use of fixed-point calibration has been fairly successful at room temperature, but is much less accurate at high temperatures.

Synchrotron radiation has been used to address some of these issues for over a decade. The change in unit cell volume under increasing pressure and temperature is measured using x-ray diffraction; the known equations of state of various materials such as NaCl and MgO are then used to determine the pressure. With the installation of the DIA multi-anvil high pressure apparatus at the superconducting wiggler beam line at the NSLS in late 1989, we perform these experiments at precisely determined temperatures on fairly large samples (~1mm^3).

In the last two years, we have developed a facility to measure acoustic velocities using ultrasonic interferometry on samples while they are under high pressure and temperature inside the DIA apparatus. The ultrasonic sample is surrounded by NaCl, which can be used to determine the pressure. In Figure G-4, we show the acoustic piezoelectric transducer-tungsten carbide anvil arrangement and the high-temperature cell assembly for the DIA. The WC anvil serves as an acoustic buffer rod to transmit the high-frequency signal (20 to 90 MHz) into the cell assembly.

Using this technique, we have measured both the compressional and shear wave velocities of most of the major components of the earth's mantle. These include magnesium silicate in the olivine[3], wadsleyite[4], garnet (majorite)[5], orthopyroxene[6], and perovskite[7] phases. Since these materials exist in the earth as Mg-Fe solid solutions, some of these measurements have been made on samples with some iron in them.

Even though the use of x-ray diffraction to determine the pressure using the equation of state of some known material is a great improvement over earlier, fixed point calibration techniques, it still depends on the knowledge of that equation of state, which was determine earlier using a variety of techniques, not all of which are necessarily very accurate. Measurement of the change in cell volume at elevated pressure (and temperature) while simultaneously measuring the P- and S-wave acoustic velocities on the same sample, provides the ability to determine the pressure absolutely without reference to earlier calibrations. The p- and s-wave acoustic velocities are given by $Vp^2=(K+(4/3)G)/\rho$ and $Vs^2=G/\rho$, where K and G are the bulk and shear moduli, respectively, and ρ is the density. These can be combined to eliminate G, giving $K=\rho[Vp^2-(4/3)Vs^2]$. Because the bulk modulus is also given by $K=VdP/dV$, these two equations can be combined to eliminate the pressure if both acoustic velocities and the cell volume (or density) are independently measured. We have begun a project making these measurements for MgO, with the goal of creating an independent pressure scale[8] ■

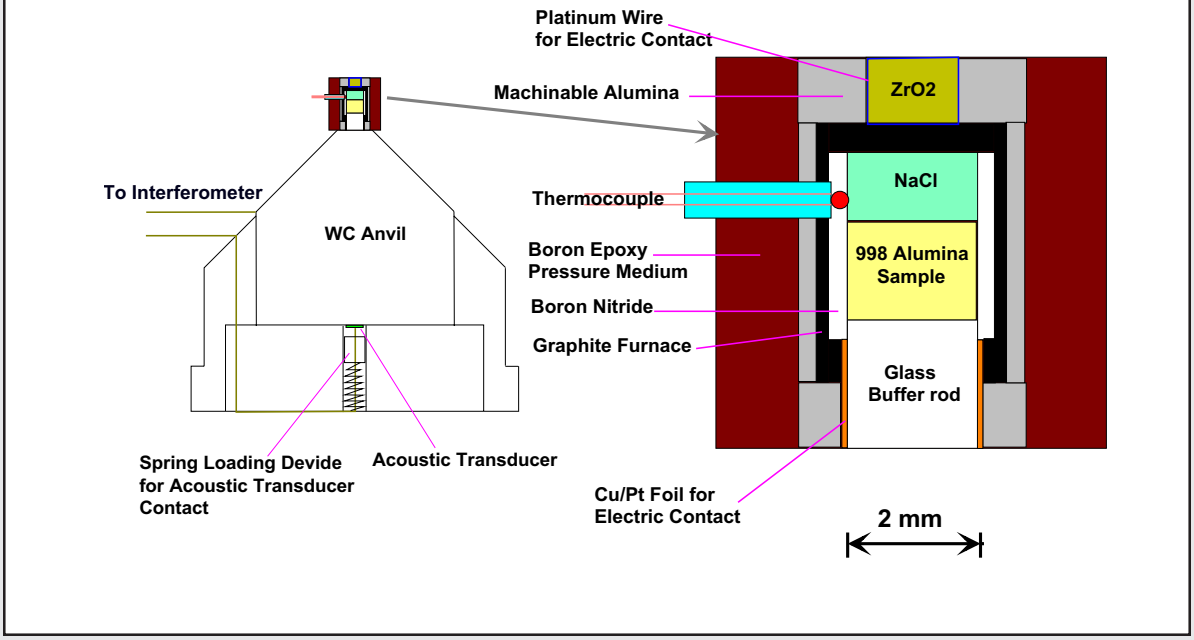

Figure G-4: Diagram of anvil insert and cell assembly for ultrasonic experiments in X17B1.

[1] G. D. Gwanmesia and R. C. Liebermann, High Pressure Research: Application to Earth and Planetary Sciences (ed. by Y. Syono and M. Manghnani), 1992.

[2] G. D. Gwanmesia, B. Li, and R. C. Liebermann, Experimental Techniques in Mineral and Rock Physics, (ed. by R. C. Liebermann and C. H. Sondergeld), PAGEOPH, 141, 467 (1993).

[3] G. Chen, Y. Sinelnikov, and R. C. Liebermann, this issue; B. Li, J. Liu, L. Flesch, R. C. Liebermann, J. Chen, and B. Savage, this issue.

[4] B. Li, J. Liu, L. Flesch, G. D. Gwanmesia, J. Chen, and R. C. Liebermann, NSLS 1996 Activity Report B-142, 1997

[5] G. D. Gwanmesia, G. Chen, Y. Sinelnikov, J. Cooke, L. Flesch, M. T. Vaughan, and R. C. Liebermann, NSLS 1996 Activity Report B-141, 1997; G. D. Gwanmesia, G. Chen, J. Cooke, L. Flesch, R. C. Liebermann, and M. T. Vaughan, this issue.

[6] L. Flesch, B.Li, J. Zhang, J. Cooke, R. C. Liebermann, and M. T. Vaughan, this issue.

[7] Y. Sinelnikov, J. Zhang, and R. C. Liebermann, NSLS 1996 Activity Report B-144, 1997; Y. Sinelnikov, J. Zhang, and R. C. Liebermann, this issue.

[8] G. Chen, Y. Sinelnikov, J. Cooke, D. J. Weidner, and R. C. Liebermann, NSLS 1996 Activity Report B-138, 1997; G. Chen, Y. Sinelnikov, R. C. Liebermann, and D. J. Weidner, this issue.

Detection of Organic Compounds Associated with Carbonate Globules and Rims in the ALH84001 Meteorite from Mars

G. J. Flynn (Dept. of Physics, SUNY-Plattsburgh), L. P. Keller, M. A. Miller (MVA, Inc.), C. Jacobsen and S. Wirick (Dept. of Physics, SUNY-Stony Brook

In August 1996, D. S. McKay and co-workers[1] reported possible evidence for biological activity on Mars in material along fracture surfaces in the ALH84001 meteorite, believed to be from Mars. They found carbonate globules, which may form by precipitation from water, along the fracture surfaces. Dark rims surrounding the carbonate globules contain magnetite and iron-sulfide grains, similar in size and shape to those produced by terrestrial bacteria[1]. They also detected organic compounds called polycyclic aromatic hydrocarbons (PAHs), frequently produced by the decay of living material, "found in the highest concentrations in the regions rich in carbonates"[1]. While each of the features might have been produced by non-biological processes, their close spatial association suggests they all formed by the same process. They concluded that biological activity, early in the Mars' history, could explain all the features[1].

Other investigators suggest the carbonates formed at high temperatures, inconsistent with precipitation from water[2]. In addition, most meteorites are contaminated by terrestrial organic matter, so the PAHs found associated with the carbonates might be from Earth not Mars. A recent study determined that a majority of the organic matter in ALH84001 is likely to be terrestrial contamination[3], although the same study found some pre-terrestrial carbon after the carbonates had been dissolved. If this carbon is organic, then 10 to 20% of the organic matter in ALH84001 was present prior to its arrival on Earth[3].

The organic measurements by McKay's group were limited by the spatial resolution of the instrument and by their ability to detect only one class of organic compounds. Their instrument has a sampling beamspot 50 microns in size[1], the width of a typical human hair. This is comparable to the size of entire carbonate globules (~50 to 100 microns), and much larger than the dark rims (~5 to 10 microns thick) or the individual magnetite crystals (tens of nanometers in size). In addition, their technique was sensitive only to PAHs, not other (possibly more interesting) organic molecules which are less stable in the laser desorption process they used.

We employed the Scanning Transmission X-Ray

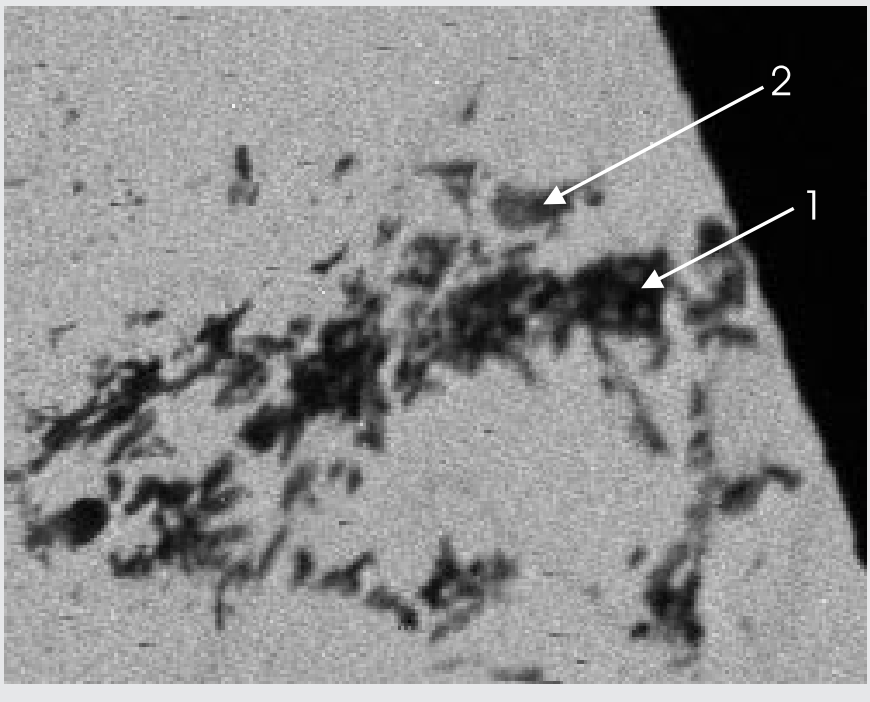

Figure G-5: STXM map of a small section of a carbonate globule from the ALH84001 meteorite. The carbon bonding state was measured at the spots indicated by the arrows.

Microscope (STXM) on beamline X1A at the National Synchrotron Light Source (NSLS) at Brookhaven National Laboratory to determine the bonding states and the spatial distribution of carbon in carbonates and rims from the ALH84001 meteorite[4]. The STXM has a 50 nanometer analysis beamspot, comparable to the size of the individual magnetite and iron-sulfide crystals, which allows the spatial association of carbon bearing compounds to be examined with a resolution about 1000 times better than that achieved by McKay and co-workers[1].

We then examined the samples using a Spectra-Tech Fourier Transform Infrared (FTIR) spectrometer, installed on beamline U4IR at the NSLS, to identify the carbon bonds[5]. Beamline U4-IR produces an intense infrared light beam, providing a sensitivity about 100 times better than the conventional laboratory FTIR instrument[6]. FTIR examination allows identification of a wide range of organic compounds, not just the PAHs detected by McKay *et al.* [1], using analysis spots down to about 3 microns in size.

Samples: Fragments of ALH84001 carbonate and rim were embedded in elemental sulfur, ultramicrotomed to ~200 nanometers thick, and deposited on an SiO substrate. This avoids exposure to the carbon-bearing epoxies and substrates normally used in preparation for Transmission Electron Microscope (TEM) and STXM examination. Thus, we insured that any carbon we detected was indigenous to the samples.

TEM examination of the carbonate samples indicated they consisted mostly of large crystals of Mg-Fe-carbonate with some regions of fine-grained Mg-Fe-carbonate and magnetite. The dark rim samples were dominated by feldspathic glass, but included large (~5 micron) chromite and a few small regions of fine-grained magnetite, sulfide, and Mg-Fe-carbonate similar to the rim material described by McKay *et al.* [1].

STXM Examination: In the STXM mapping mode, the energy of the incident monochromatic x-ray beam is fixed and the sample is scanned beneath the beam. The

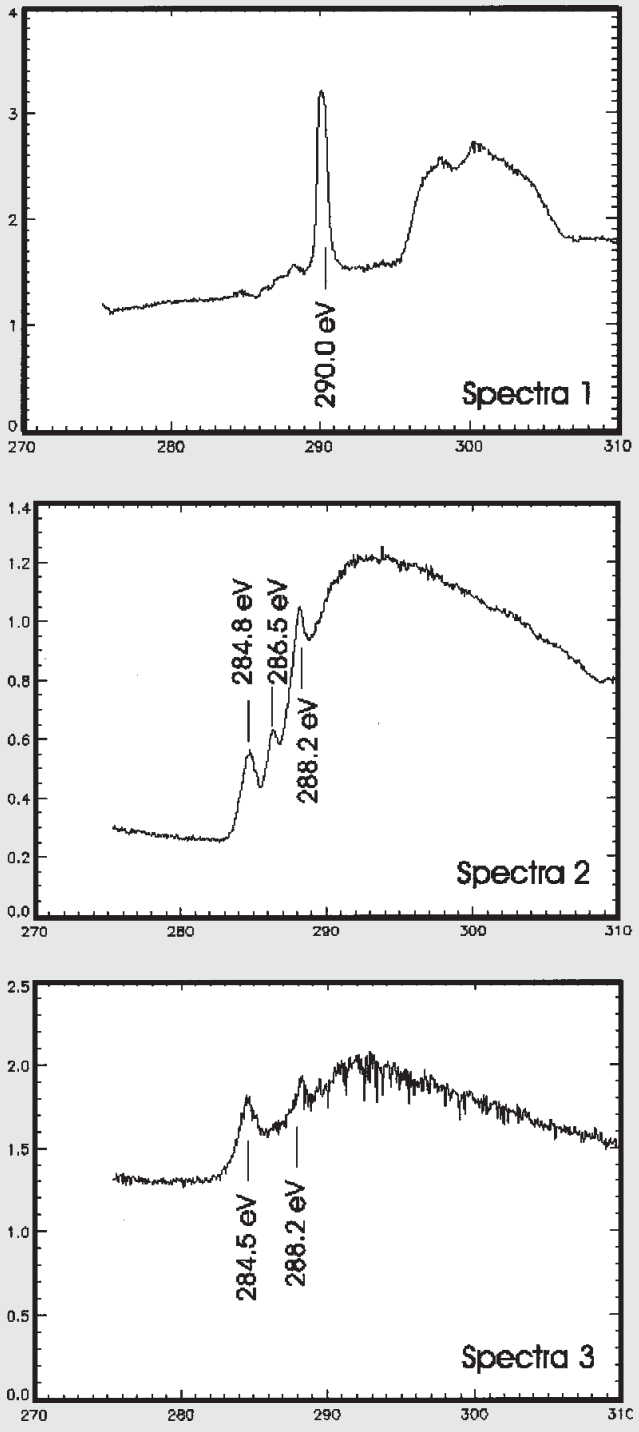

Figure G-6: Carbon-XANES spectra of two spots (shown in Figure G-5) on a carbonate globule from ALH84001. Spot 1 has a strong absorption at 290 eV, indicating the carbon is bound in carbonate, while Spot 2 has three absorptions, at 284.9, 286.5, and 288.2 eV, suggesting the presence of orrganic carbon at this spot. Spot 3 is a carbon-rich spot on the rim sample. It shows strong absorptions at 284.5 and 288.2 eV, indicating the rim contains a different type of carbon than that in the globule.

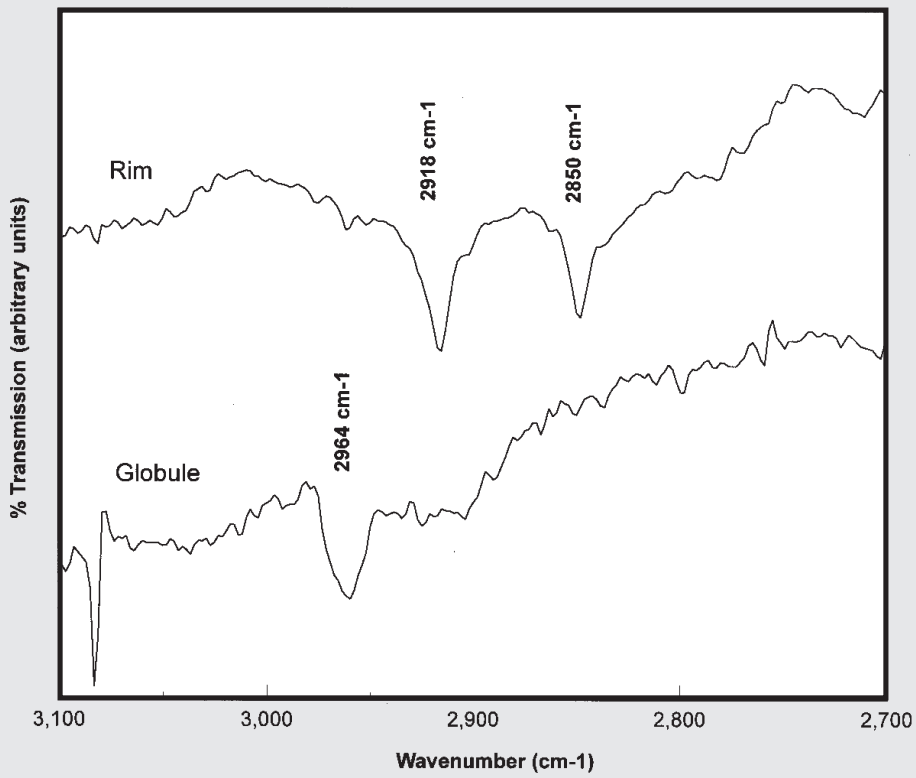

Figure G-7: FTIR spectra of the C-H stretching region of a Rim sample (top) and a Carbonate Globule sample (bottom) from the ALH84001 meteorite. The Rim sample shows two strong absorptions, at 2918 and 2850 cm^{-1}, consistent with the positions and relative intensities of the $C-H_2$ stretching vibrations in an aliphatic hydrocarbon. The Carbonate Globule sample shows a single strong absorption at 2964 cm^{-1}, consistent with a $C-H_3$ stretching vibration, and a weaker, broad absorption from 2900 to 2950 cm^{-1}. This sample may also show a very weak, broad feature from 2990 to 3060 cm^{-1}, possibly associated with PAHs.

absorption of the sample is measured at each pixel. Since the absorption of carbon increases sharply at 290 eV, the carbon K-edge energy, while the absorptions of other elements are approximately constant in a narrow range of energy near the carbon K-edge, a pixel showing an increase in absorption between the map just below the carbon K-edge (e.g., 280 eV) and the map just above the carbon K-edge (e.g., 300 eV) contains carbon (see image in Figure G-5).

In Carbon-X-ray Absorption Near Edge Structure (C-XANES) mode the beam hits a fixed position on the sample, and the monochrometer is scanned over the energy range from 270 to 310 eV. Absorptions in this region are characteristic of particular carbon bonds. The C-O bond in carbonate gives rise to a strong absorption near 290 eV but no absorption near 285 eV, while C-C, C=C, and C-H bonds have strong absorptions in the 284 to 287 eV range. Thus, C-XANES is a sensitive technique to detect organic (or graphitic) carbon in a matrix of carbonate, making the STXM particularly well suited to identifying non-carbonate carbon in a matrix of carbonate (as is the case for the ALH84001 carbonate and rim samples).

The C-XANES spectra of the carbonate samples showed a strong absorption at 290 eV, characteristic of the C-O bond in carbonate. These samples also showed weaker absorptions at 284.8 eV, 286.5 eV, and 288.2 eV (see Figure G-6). The relative intensities of the latter three absorption peaks were approximately constant (where they could be detected), suggesting that throughout the carbonate samples a single additional carbon-bearing phase dominated the absorption. However these three peaks varied in intensity with position on the sample, ranging from spots showing only

the 290 eV carbonate peak to spots showing strong absorptions at 284.8 eV, 286.5 eV, and 288.2 eV but no detectable 290 eV peak. This indicates the second carbon-bearing phase is distributed inhomogeneously, on the scale of the 50 nm beamspot, within the carbonate. Work is in progress to correlate the locations of this phase with TEM mineralogy.

Most spots on the rim samples showed no absorption at 290 eV, consistent with a low abundance of carbonate. Some spots showed two absorption peaks at 284.5 eV and 288.2 eV, indicating the presence of C-C, C=C, C-O, or C-H bonds. The differences in absorption energies and the absence of the third peak in indicate that the dominant carbon-bearing phase in the rim is different from that in the carbonate globule. Correlation of the STXM carbon map with TEM mineralogy indicates the carbon-rich phase is associated with fine-grained magnetite and sulfide, and may also occur as veins or inclusions in the feldspathic glass.

FTIR Examination: To determine if the dominant carbon-bearing compound is different in the rim samples and the carbonate globule samples and to determine if these phases are organic, the same samples analyzed by STXM were examined by FTIR, a technique routinely used for the laboratory identification of organic compounds. The FTIR spectra of the rim samples showed a broad absorption near 1000 cm^{-1}, characteristic of silicate glass, and two weaker features at 2918 cm^{-1} and 2850 cm^{-1}, consistent in position and relative depths with the stretching vibrations of $C-H_2$ in an aliphatic hydrocarbon (see Figure G-7).

The FTIR spectra of the carbonate globule samples showed a narrow absorption at ~1500 cm^{-1}, characteristic of carbonate, and a weaker absorption at 2964 cm^{-1}. The feature at 2964 cm^{-1} is characteristic of the $C-H_3$ asymmetrical stretching vibration. Although a weaker $C-H_3$ symmetrical stretching vibration generally occurs near 2870 cm^{-1}, this feature is absent in the carbonate globule spectrum, and is suppressed in certain compounds containing $C-H_3$ groups. Two even weaker features at 2920 cm^{-1} and 2850 cm^{-1}, consistent with $C-H_2$, were also detected at some spots on the carbonate globule samples. One particularly good spectrum of the carbonate globule sample appears to show a weak, broad absorption over the range 2990 cm^{-1} and 3060 cm^{-1}, where the C-H stretching vibrations (centered at 3030 cm^{-1}) of a mixture of PAHs would occur. Follow-up measurements to determine if we have located the PAHs are planned.

Conclusions: The combined STXM and FTIR measurements confirm, at a much smaller scale than was possible in the work of McKay *et al.* [1], the close spatial association between organic material and the carbonate globules and rims in ALH84001. The carbon detection limit of the STXM is of order percent level. If ALH84001 has a similar bulk carbon content other Mars meteorites (0.04 to 0.07%[7]), then the STXM results demonstrate that compared to the bulk meteorite relatively large concentrations of organic carbon are associated with the carbonate globules and rims. The FTIR measurements indicate the rim material contains an aliphatic hydrocarbon whose absorption is dominated by the $C-H_2$ group, while the carbonate globule is dominated by the $C-H_3$ group absorption. Thus the rim and the globule contain different organic compounds. This results seems to rule out the simplest form of organic contamination of these samples, simple evaporation of an organic-rich fluid, which would be expected to leave the same residue in both the carbonate globules and the adjacent rim material. However, we cannot exclude contamination by selective absorption of different organic species onto the different mineral substrates. ■

[1] D.S. McKay *et al., Science* **273**, 924-927 (1996).
[2] R. Harvey and H.P. McSween, *Nature*, 382, 49ff, (1996).
[3] A.J.T. Jull *et al., Science* **279**, 366-369, (1998).
[4] G.J. Flynn *et al., Meteoritics* **32**, A42, 1997.
[5] G.J. Flynn *et al., Lunar & Planetary Science XXIX, Lunar and Plantetary Institute,* (1998), in press.
[6] J. Reffner *et al., Synchrotron Radiation News* **V. 7**, 30-37 (1994).
[7] A.H. Tremain, *Geochem. Cosmochim. Acta* **50**, 1071-1091 (1986).